

Supplementary Information

Quantum Efficiency Optimization by Maximizing Wave Function Overlap in Type-II Superlattice Photodetectors

Yunhao Zhao, Lu Liu, Han Bi, Xi Han, Xuebing Zhao, Haiqiao Ni, Yingqiang Xu, Zhichuan Niu, Renchao Che*

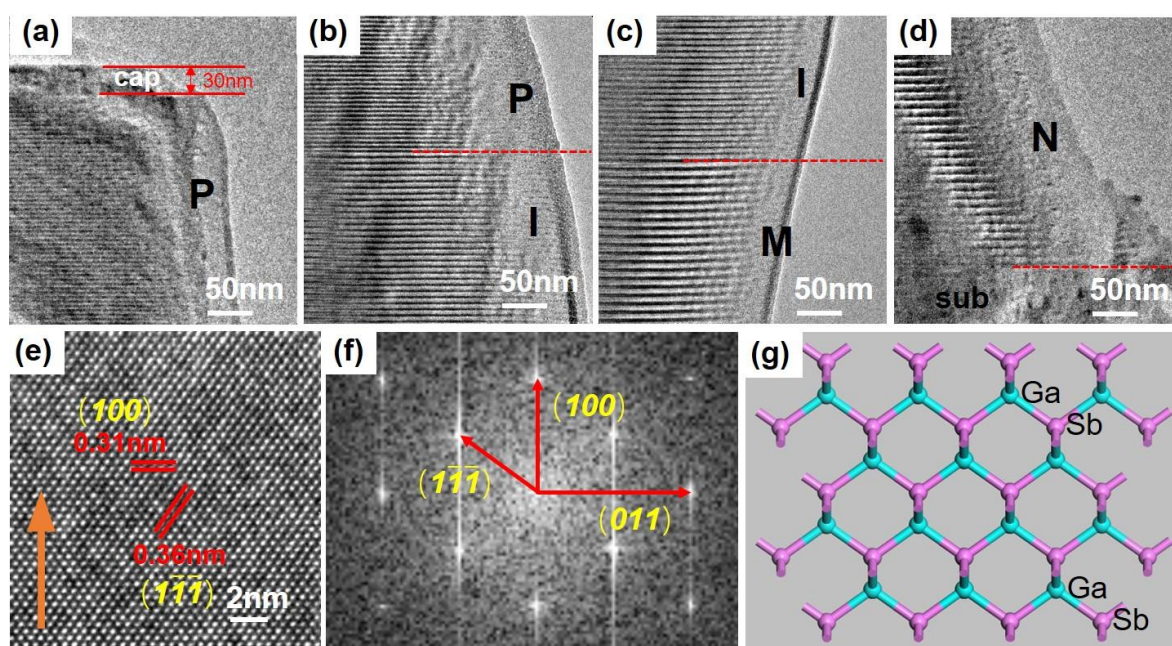


Figure S1. TEM images of our PIMN photodetector. (a) the cap layer and the P-doped region; (b) the P-I interface; (c) the I-M interface and (d) the N-sub interface. (e) HRTEM of the (100) GaSb substrate. The inserted orange arrow gives the MBE growth direction. (f) fast Fourier transformation of (e) indicating the crystal plane index. (g) atomic structure corresponding to the GaSb substrate in (e).

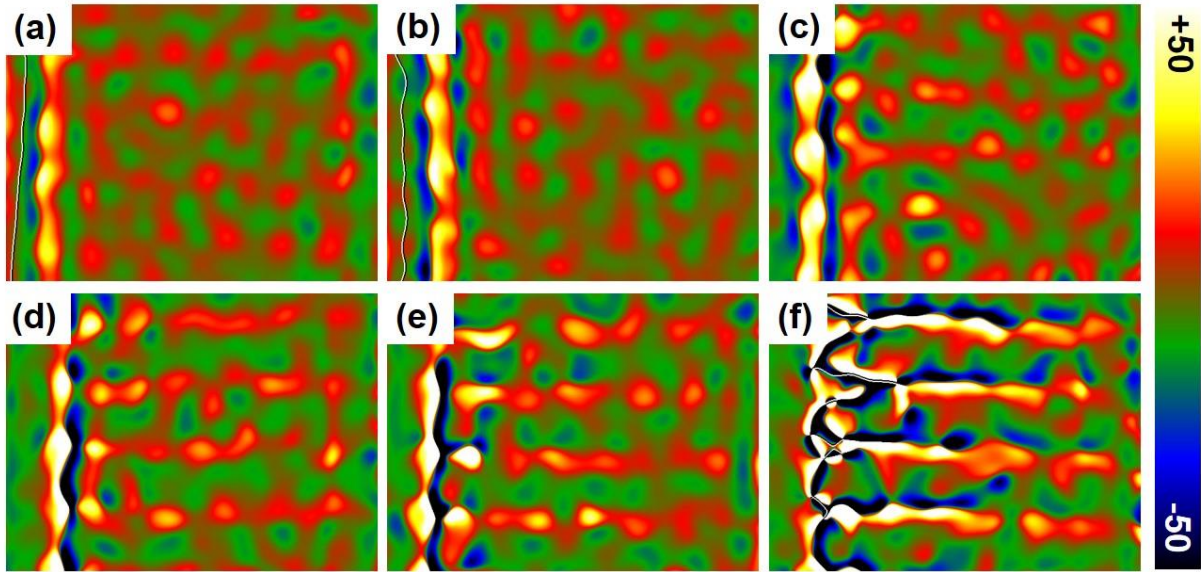


Figure S2. Charge density maps of the absorption region under different voltages in PIMN T2SL infrared detector. Charge density maps under different voltages: (a) 0 mV; (b) 1500 mV; (c) 3000 mV; (d) 3500 mV; (e) 4000 mV and (f) 4500 mV. Uniform color marker of (a) to (f) on the right side shows the charge density range from -50 e/nm^3 to 50 e/nm^3 .

As shown in the pictures, charge distribution seems not so clear as period until the voltage goes to 3000 mV. Profiles of charge density maps of low voltage series (0 mV, 1500 mV and 3000 mV) and high voltage series (3500 mV, 4000 mV and 4500 mV) will be shown as the following Fig. S3.

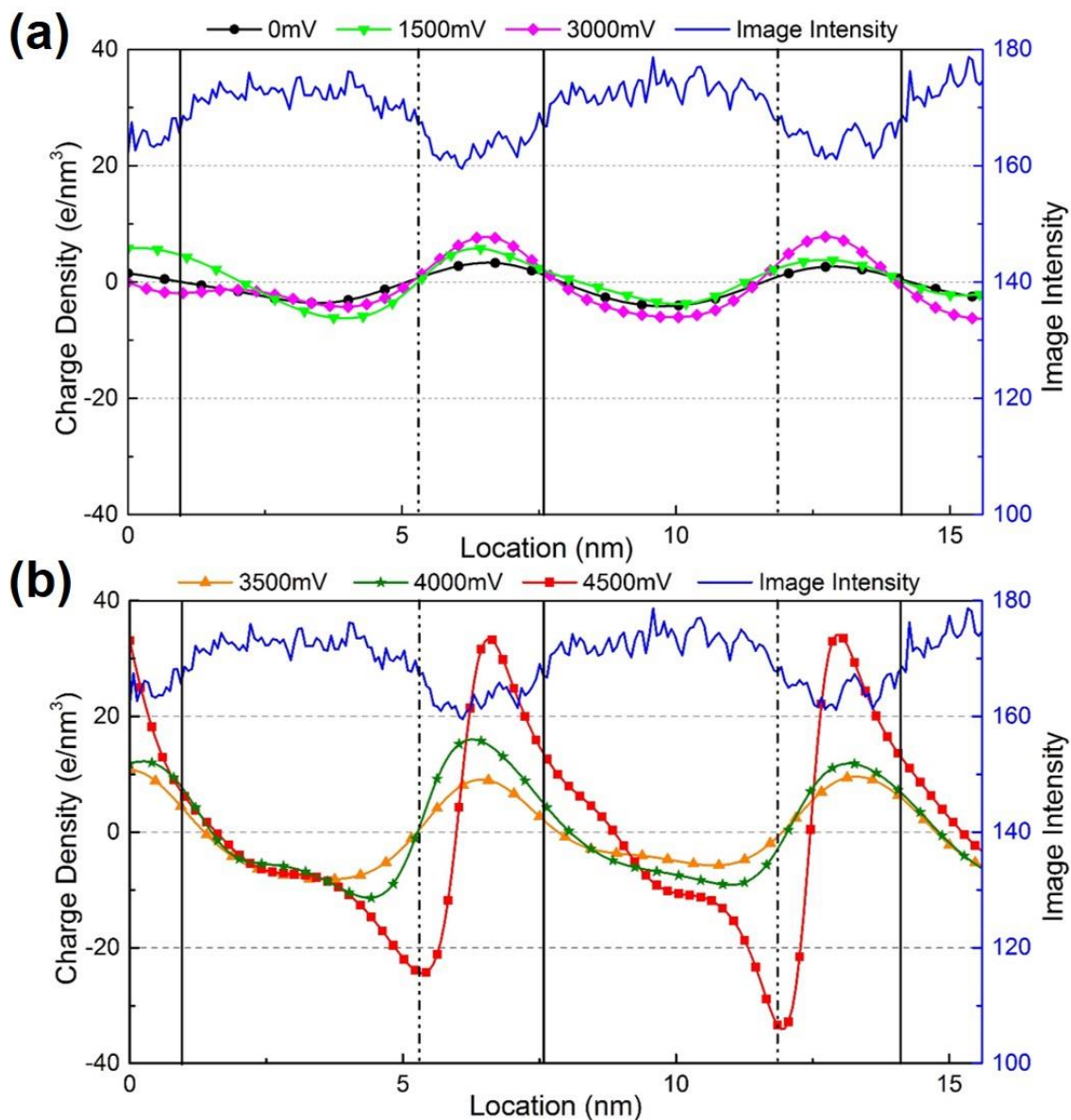


Figure S3. Profiles of charge density maps under the lower series of voltages and the higher series of voltages. (a) the profiles of Fig. S2a,b,c and the corresponding image intensity of one hologram. (b) the profiles of Fig. S2d,e,f and the corresponding image intensity of one hologram.

The shapes of the curves in Fig. S3a do not vary a lot except some change in intensity, which indicates an even distribution of charge under weak electric field. However, in Fig S3b, shape changes greatly with voltage increasing.

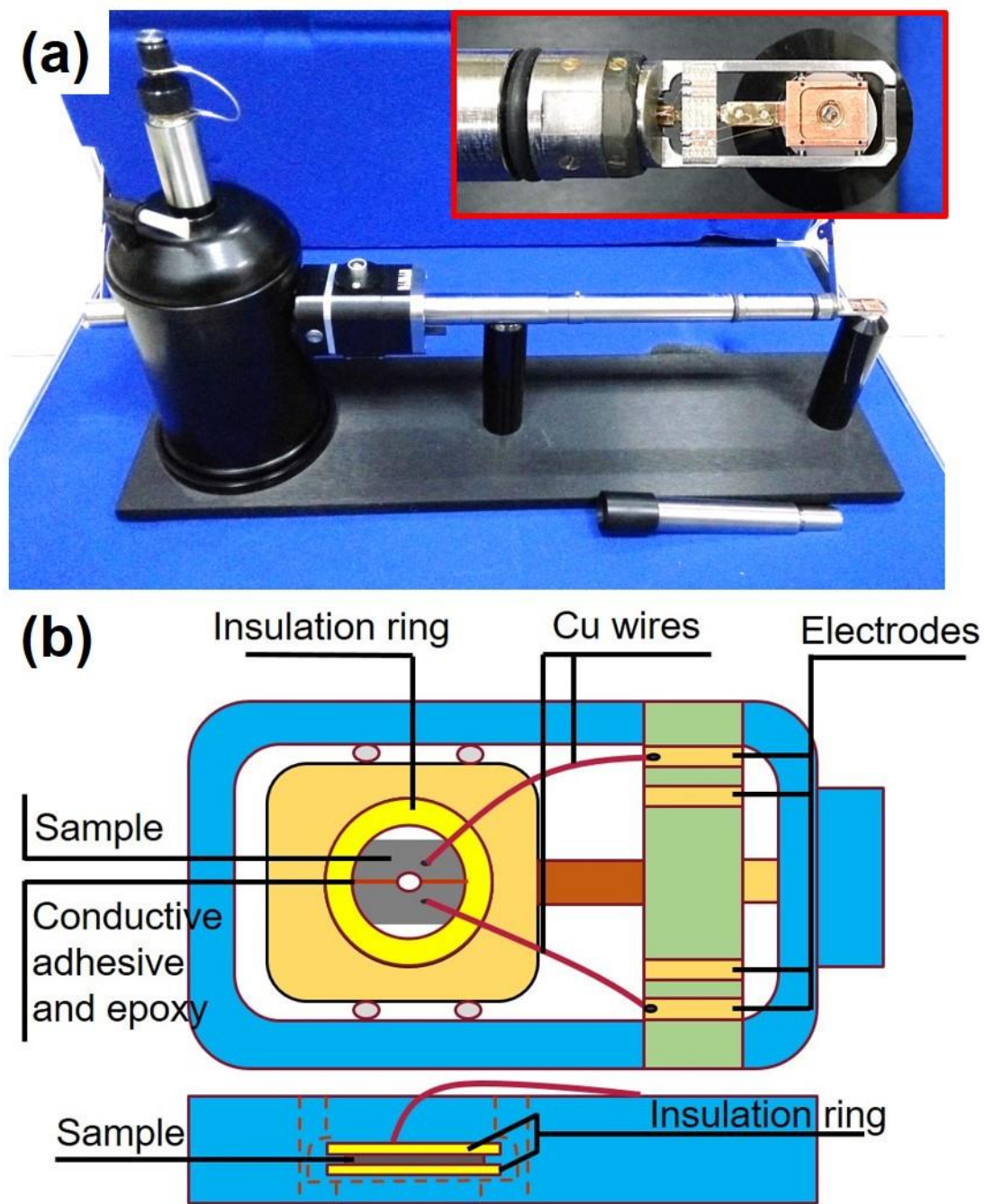


Figure S4: Pictures and schematic diagrams of the sample holder used in our *in situ* TEM experiments. (a) the TEM sample holder used in our experiment. The inset at the corner gives a closer view of the tip of the holder. (b) a schematic diagram of the *in situ* bias platform shown in (a).

Methods

Growth and characterization of the PIMN type-II superlattice infrared detector: The type-II superlattice infrared detector with PIMN structure was grown by MBE on GaSb (100) substrate. Deoxidizing was first performed on the substrate at 560 °C (833 K) and followed by degassing at 620 °C (893 K) for 10 min to remove the contamination. Then GaSb buffer layer of about 1 μ m was grown within 90 min at 545 °C (818 K). After that, PIMN structure was grown on the buffer layer as shown in Table 1. Finally, a 30 nm GaSb cap was grown at 950 °C for 200 s to cover and protect the structure below it. It is worth noting that in order to make the superlattice ideal as predesigned, InSb was used to modulate the interface during growth to obtain the sharp and clear interface. QE was obtained after the material had been encapsulated into a detector device.

Table 1. Growth information of T2SL infrared detector with PIMN structure.

Layer	Region	Materials in single period and doping element(ML: monolayer)	Thickness(nm)	Doping concentration(cm^{-3})	Doping type
7	Cap	GaSb(Be)	30	3×10^{18}	P
6	P contact	8ML InAs/8ML GaSb(Be)	342	3×10^{18}	P
5	Absorption	15ML InAs/8ML GaSb	4000	10^{15}	I
4	M structure barrier	19ML GaSb/5ML GaSb InAs(Si)/4ML InAs/3ML GaSb	495	2×10^{18}	N
3	N contact	19ML GaSb/5ML GaSb InAs(Si)/4ML InAs/3ML GaSb	495	2×10^{18}	N
2	Buffer layer	GaSb	1000	10^{18}	N
1	Substrate	GaSb	600(μm)	10^{17}	N

Measurement of in situ bias electron holography: Samples for TEM test were prepared by mechanical polish and ion milling. After that, the sample attached to an isolated $\phi 3$ copper ring was anchored on the Gatan in situ sample platform while two isolated ring were set both on and under the sample to guarantee the isolation between the sample and the platform. Manually, we fixed Cu wire by silver conducting adhesive as electrodes on the GaSb substrate of both sides of the sample (Fig. S4). Holography biprism was fixed in JEOL-2100F field emitting transmission electron microscope. Charge-coupled device camera was equipped to record holograms. Before the test, direction of the applied voltage was determined according to the direction of the voltage under working condition. During the test, the biprism was biased to 40 V. Certain voltages were applied on the sample using Protochip Audro 500 power source and holograms were captured while the voltage is fixed for several seconds. The amplification of the TEM was chosen as 200k to maintain enough resolution on one hand and to avoid lattice fringes which might have influence on the subsequent processing and analysis on the other hand. Spot 3 and 3# condenser aperture were also carefully selected to protect the sample from being damaged too soon by the electron beam.

Data processing for electron holography: The reference hologram was recorded through vacuum before or after in situ bias test without any applied voltage on the sample to avoid the effect of stray field. From the sideband location (3.22 1/nm from the center) in FFT image of the reference, we can get a resolution of about 0.31 nm. With the help of a plug-in HoloWork attached in Digital Micrography of Gatan, we are able to do reconstruction and even unwrapping to achieve phase images and amplitude images. We take a relatively small radius for reconstructing to improve the signal to noise ratio.

Formulations used to obtain electric potential from phase images are shown as

$$\Delta\varphi(x, y) = C_E \cdot \int \{V_0(x, y, z) + V_{bi}(x, y, z)\} dz \quad (1)$$

Where V_0 is the mean inner potential of materials and V_{bi} is the built-in potential caused by charge distribution while C_E is an electron-energy-dependent interaction constant with the value of $7.28 \times 10^{-3} \text{ V}^{-1} \cdot \text{nm}^{-1}$ for electrons with energy of 200 keV in our experimentation.

Investigations on amplitude images demonstrate that a similar constant thickness can be used to simplify Equation 1 to

$$\Delta\varphi(x, y) = C_E \cdot \{V_0(x, y) + V_{bi}(x, y)\} \cdot t \quad (2)$$

Where t is the sample thickness taken as 30 nm during data processing.

Poisson equation,

$$\nabla^2 V_{bi} = -\rho / \varepsilon_0 \varepsilon_r \quad (3)$$

was finally used to get charge density maps. ε_0 is the dielectric constant in vacuum ($\sim 8.854 \times 10^{-12} \text{ F/m}$) and ε_r is the relative dielectric constant of materials.

It has to be clarified that while GaSb and InAs in our superlattice sample have different V_0 (15.506 and 15.569 respectively) and ε_r (15.7 and 15.1 respectively), we unify them (15.537 for V_0 and 15.4 for ε_r) to facilitate our calculation in MATLAB based on three following facts. Firstly, the period of the superlattice are so short that it's not appropriate to distinct all the composition layers by sharp interfaces as sharp interfaces are nearly impossible in actual material growth process. The second fact is that different constant used at sharp interfaces could induce abnormal values especially when differential is operated. At last, differences between the constants could only have influence on shape of curves and are small enough to not introduce severe errors into our results as we focus mostly on the distribution but not the intensity on charge densities. Therefore, it's reasonable to use the unified eclectic parameters to deal with our diagrams.